11. D. M. Veine, K. Ohnishi, C. H. Williams Jr., *Protein Sci.* **7**, 369 (1998).
12. D. M. Veine, S. B. Mulrooney, P.-F. Wang, C. H. Williams Jr., *Protein Sci.* **7**, 1441 (1998).
13. See the animation at *Science* Online (www.sciencemag.org/feature/data/1051414.shl).
14. The C4 atom of $AADP^+$ and the N5 atom of FAD are separated by 3.4 Å (*7*).
15. The structure of glutathione reductase was used by Kuriyan and co-workers (*2*) to predict the domain packing in the FR structure of TrxR. They aligned the FAD domains of glutathione reductase and TrxR and then matched the NADPH domain of TrxR to the corresponding domain of glutathione reductase. The rotation applied to the NADPH domain to build the model (66°) is almost identical to the observed rotation, but the core main-chain atoms of the modeled NADPH domain are displaced from those observed in our structure by a root mean square deviation of 4.9 Å.
16. S. Hayward and H. J. C. Berendsen, *Proteins* **30**, 144 (1998).
17. Hydrogen bonds and ion pairs were assigned by the program CONTACTS (*29*). In both the FO and FR structures, two protein-protein hydrogen bonds connect the FAD and NADPH domains of the same monomer chain. In the FO structure, eight hydrogen bonds link the NADPH domain of one monomer to the FAD domain of its partner chain; only three such interactions are found in the FR structure. There are similar numbers of well-ordered waters in the domain interfaces (17 for the FO, 21 for the FR conformation).
18. G. E. Schulz, *Curr. Opin. Struct. Biol.* **1**, 883 (1991).
19. M. Gerstein *et al.*, *J. Mol. Biol.* **234**, 357 (1993).
20. M. Gerstein and W. Krebs, *Nucleic Acids Res.* **26**, 4280 (1998).
21. M. Lesk and C. Chothia, *Nature* **335**, 188 (1988).
22. O. Herzberg *et al.*, *Proc. Natl. Acad. Sci. U.S.A.* **93**, 2652 (1996).
23. The average temperature factor, $\langle B \rangle$, for the thioredoxin chains, ~80 $Å^2$, is much larger than $\langle B \rangle$ for the rest of the cross-linked complex (Table 1), but the residues at the interfaces with TrxR are more ordered ($\langle B \rangle$ = 63 $Å^2$).
24. H. Eklund, F. K. Gleason, A. Holmgren, *Proteins* **11**, 13 (1991).
25. H. Eklund *et al.*, *EMBO J.* **3**, 1443 (1984).
26. E. F. Pai and G. E. Schulz, *J. Biol. Chem.* **258**, 1752 (1983).
27. L. D. Arscott, S. Gromer, R. H. Schirmer, K. Becker, C. H. Williams Jr., *Proc. Natl. Acad. Sci. U.S.A.* **94**, 3621 (1997).
28. T.-W. Gilberger, B. Bergmann, R. D. Walter, S. Müller, *FEBS Lett.* **425**, 407 (1998).
29. Collaborative Computational Project No. 4, *Acta Crystallogr.* **D50**, 760 (1994).
30. C. H. Williams Jr., *FASEB J.* **9**, 1267 (1995).
31. L. Thelander and P. Reichard, *Annu. Rev. Biochem.* **48**, 133 (1979).
32. D. F. Mark and C. C. Richardson, *Proc. Natl. Acad. Sci. U.S.A.* **73**, 780 (1976).
33. M. Carson, *Methods Enzymol.* **277**, 493 (1997).
34. Z. Otwinowski and W. Minor, *Methods Enzymol.* **276**, 307 (1997).
35. L. Tong and M. G. Rossmann, *Methods Enzymol.* **276**, 594 (1997).
36. H. M. Doesburg and P. T. Beurskens, *Acta Crystallogr.* **A39**, 368 (1983).
37. T. A. Jones, J. Y. Zou, S. W. Cowan, M. Kjeldgaard, *Acta Crystallogr.* **A47**, 110 (1991).
38. We thank D. M. Veine for purification of the $Cys^{35} \rightarrow$ Ser mutant of thioredoxin. Supported by NIH fellowship award GM18723 (B.W.L.) and by NIH grants GM16429 (M.L.L.) and GM21444 (C.H.W.). Coordinates for this structure have been deposited in the Protein Data Bank (accession code 1F6M).

17 April 2000; accepted 30 June 2000

Asef, a Link Between the Tumor Suppressor APC and G-Protein Signaling

Yoshihiro Kawasaki,[1] Takao Senda,[2] Takao Ishidate,[1] Ryo Koyama,[1] Tsuyoshi Morishita,[1] Yoriko Iwayama,[2] Osamu Higuchi,[1] Tetsu Akiyama[1,3]*

The *adenomatous polyposis coli* gene (*APC*) is mutated in familial adenomatous polyposis and in sporadic colorectal tumors. Here the APC gene product is shown to bind through its armadillo repeat domain to a Rac-specific guanine nucleotide exchange factor (GEF), termed Asef. Endogenous APC colocalized with Asef in mouse colon epithelial cells and neuronal cells. Furthermore, APC enhanced the GEF activity of Asef and stimulated Asef-mediated cell flattening, membrane ruffling, and lamellipodia formation in MDCK cells. These results suggest that the APC-Asef complex may regulate the actin cytoskeletal network, cell morphology and migration, and neuronal function.

Mutations of the tumor suppressor gene *APC* are responsible for familial adenomatous polyposis, a dominantly inherited disease characterized by multiple adenomatous polyps in the colon (*1*). The *APC* gene is also somatically mutated in most sporadic colorectal tumors. Consistent with its role as a tumor suppressor, overexpression of *APC* blocks cell cycle progression from the G_1 to S phase (*2*). The product of the *APC* gene interacts with various proteins, including β-catenin, a key component of the Wnt/Wingless signaling transduction pathway that plays important roles in a number of developmental processes and in tumorigenesis (*3*). APC is thought to be involved in the degradation of β-catenin through its interaction with β-catenin, GSK-3β, and Axin or the closely related factor conductin/Axil (*4*). APC also interacts with EB1 and the human homolog of the *Drosophila* Discs large (hDLG) through its COOH-terminal region (*5*, *6*). Furthermore, APC possesses an armadillo repeat domain, which is thought to be involved in protein-protein interactions. To obtain new insights into the function of APC, we attempted to identify proteins that interact with the armadillo repeat domain of APC.

We screened a human fetal brain library using the armadillo repeat domain of APC as target, and isolated a gene that we have named *Asef* (for APC-stimulated guanine nucleotide exchange factor) (*7*). The human full-length *Asef* cDNA encodes a protein of 619 amino acids with motifs found in the Dbl family of proteins (Fig. 1, A and B) (*8*). Asef contains the Dbl homology (DH), Pleckstrin (PH), and Src homology 3 (SH3) domains. Northern blot analysis of Asef revealed a mRNA of 3.6 kb that is highly expressed in mouse brain (*9*).

To confirm that APC and Asef interact directly, we created a fusion protein (APC-arm) consisting of the armadillo repeat domain of APC and glutathione-*S*-transferase (GST). We examined the ability of this fusion to interact with the fragment of Asef (Asef-M in Fig. 2A) (*10*). The in vitro–translated APC-arm interacted with GST–Asef-M, but not with GST alone (Fig. 2B). Likewise, in vitro–translated Asef-M interacted with GST–APC-arm, but not with the armadillo repeat domain of β-catenin fused to GST (GST–β-catenin–arm) or GST alone.

To identify the region of Asef responsible for its interaction with APC, we performed two-hybrid assays using deletion fragments of Asef. Mutants lacking amino acids 73 to 126 were negative for interaction with APC, whereas a fragment containing amino acids 73 to 126 was positive (Fig. 2A). This indicates that the APC-binding region may reside in the NH_2-terminal region upstream of the SH3 domain.

We next examined whether endogenous Asef associates with APC in vivo. A lysate from embryonic rat brain was subjected to immunoprecipitation with antibodies to Asef (anti-Asef) followed by immunoblotting with anti-APC (*11*). Asef was identified as an 85-kD protein and coimmunoprecipitated with APC (Fig. 2C). Similarly, immunoprecipitation of the lysate with anti-APC followed by immunoblotting with anti-Asef revealed an association between APC and Asef. Coprecipitation of Asef and APC was inhibited by preincubation of the antibodies with

[1]Laboratory of Molecular and Genetic Information, Institute for Molecular and Cellular Biosciences, University of Tokyo, 1-1-1 Yayoi, Bunkyo-ku, Tokyo 113, Japan. [2]Department of Anatomy I, Nagoya University School of Medicine, 65 Tsurumai-cho, Showa-ku, Nagoya, Aichi 466, Japan. [3]Department of Oncogene Research, Institute for Microbial Diseases, Osaka University, 3-1 Yamadaoka, Suita, Osaka 565, Japan.

*To whom correspondence should be addressed. E-mail: akiyama@imcbns.iam.u-tokyo.ac.jp

the antigens used for immunization. Immunoblot analysis of the Asef immunoprecipitates with anti–β-catenin revealed that β-catenin also coimmunoprecipitates with Asef. In addition, Asef was detected in β-catenin immunoprecipitates. Because Asef does not interact directly with β-catenin (Fig. 2B), these findings suggest that Asef, APC, and β-catenin are contained in the same complex in vivo.

Consistent with the finding that APC interacts with Asef, immunohistochemical analysis with anti-APC and anti-Asef showed that both APC and Asef are expressed in mouse colon epithelial cells (Web figure 1) (*12*, *13*). Asef is highly expressed in the central nervous system, including the hippocampus, olfactory bulb, and cerebellum, where APC is also highly expressed (*14*, *15*). Both APC and Asef localized in the cytoplasm of the hippocampal pyramidal neurons (Web figure 2) (*12*) and in the olfactory glomeruli (Web figure 1) (*12*). Double-labeling immunoelectron microscopy revealed colocalization of APC and Asef in the synapse of the olfactory glomerulus (Web figure 1) (*12*, *16*).

The Dbl family of proteins are guanine nucleotide exchange factors (GEFs) for specific members of the Rho family of small GTP-binding proteins (G proteins) (*8*). We found that Rho and Rac, but not Cdc42, bound to His_6-tagged-Asef (His_6-Asef) immobilized to ProBond Resin (Fig. 3A) (*17*). In contrast, Dbl associated with all three of these proteins, as reported previously (*18*). This suggests that Asef may function as a GEF for Rac and Rho, but not Cdc42. However, when full-length Asef was incubated with Rac bound to [^{3}H]GDP, it stimulated dissociation of GDP from Rac only very weakly (Fig. 3B) (*19*). Because many proteins of the Dbl family exhibit oncogenic activity when their NH_2-terminal regions are truncated (*8*), we reexamined GEF activity using a mutant form of Asef lacking the NH_2-terminal region (AsefΔAPC). This region contains the APC-binding domain of Asef. As expected, AsefΔAPC strongly stimulated dissociation of GDP from Rac in a time- and dose-dependent manner (Fig. 3, B and C). In contrast, mutant AsefΔAPC that also lacked the DH domain did not show this activity (*9*). AsefΔAPC stimulated binding of [^{35}S]GTPγS to Rac (*9*), but did not affect the GEF activity of Rho and Cdc42 (Fig. 3C). These results suggest that Asef has the potential to function as a GEF specific for Rac, and that this activity is negatively regulated by its NH_2-terminal region, which contains the APC-binding domain.

We next investigated whether APC affects the Rac-specific GEF activity of Asef. When added to GEF assay reaction mixtures, GST-APC-arm but not GST alone, stimulated the activity of the full-length Asef in a dose-dependent manner and to a level comparable to that achieved with AsefΔAPC (Fig. 3, B and D). Thus, APC may activate the GEF activity of Asef by binding to its NH_2-terminal region and relieving negative regulation.

Rac is involved in the reorganization of the actin cytoskeletal network, producing lamellipodia and membrane ruffling (*20*). We therefore examined the effect of Asef on the morphology of MDCK cells (*21*). When the cells were transfected with the full-length *Asef*, they became flattened onto the substratum and exhibited membrane ruffles and lamellipodia (Fig. 4A). However, when the APC-binding region of Asef was exogenously expressed along with the full-length Asef, these morphological changes were not observed (Fig. 4, G to J). Thus, we believe these morphological changes are induced by Asef that is activated by interaction with endogenous APC. Furthermore, when the

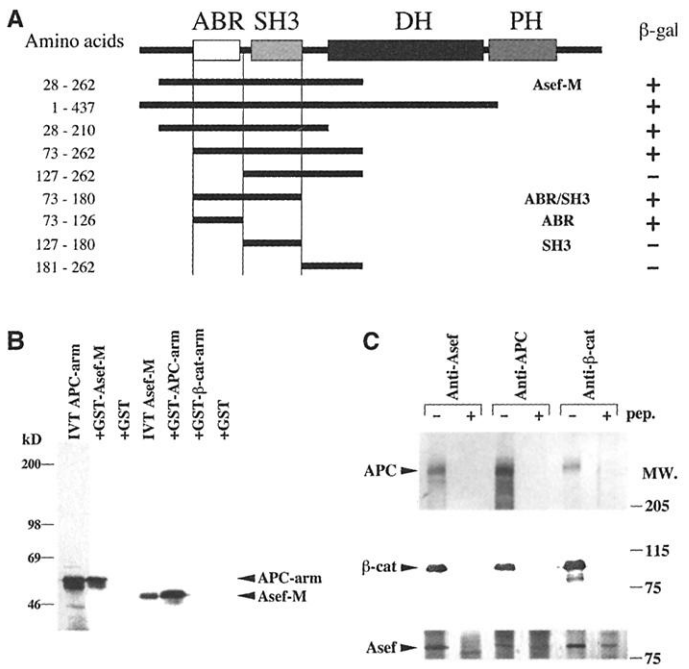

Fig. 2. Association of Asef with APC in vitro and in vivo. **(A)** Mapping of the regions in Asef required for binding to APC. Deletion constructs of Asef were analyzed for their ability to interact with APC in the two-hybrid system. (+) Detectable activity; (−) no detectable activity; Asef-M, the fragment of Asef isolated in the initial two-hybrid screen. **(B)** Association of Asef with APC in vitro. In vitro–translated (IVT) ^{35}S-labeled APC-arm was incubated with GST–Asef-M or GST-Sepharose. In vitro–translated ^{35}S-labeled Asef-M was incubated with GST–APC-arm, GST–β-catenin–arm, or GST-Sepharose. Bound proteins were analyzed by 10% SDS-PAGE and fluorography. **(C)** Association of Asef with APC and β-catenin in vivo. Lysates prepared from embryonic rat brain were subjected to immunoprecipitation with the indicated antibodies, then were fractionated by 6% SDS-PAGE and immunoblotted with the indicated antibodies. Pep (+) indicates that antibodies were preincubated with antigen before use in immunoprecipitation. GST–β-catenin was used to block anti–β-catenin.

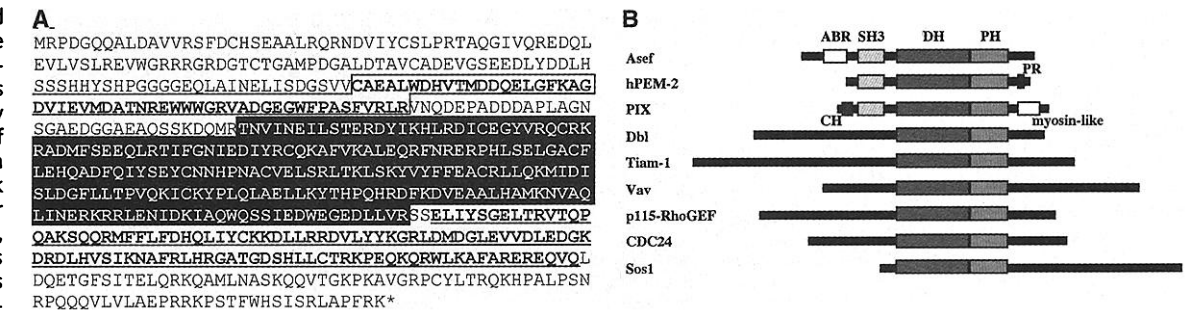

Fig. 1. **(A)** Predicted amino acid sequence of Asef and **(B)** alignment of homologous domains in Dbl family members. The Asef sequence has been deposited in GenBank (accession number AB042199). In (A), the SH3 domain is shown in bold and is boxed, the DH domain is highlighted in black, and the PH domain is shown in bold and underlined. ABR, APC-binding region; PR, proline-rich region; CH, calponin homology domain. Abbreviations for the amino acid residues are as follows: A, Ala; C, Cys; D, Asp; E, Glu; F, Phe; G, Gly; H, His; I, Ile; K, Lys; L, Leu; M, Met; N, Asn; P, Pro; Q, Gln; R, Arg; S, Ser; T, Thr; V, Val; W, Trp; and Y, Tyr.

cells were transfected with the full-length *Asef* along with *APC-arm*, they became enlarged and exhibited even more abundant membrane ruffles and lamellipodia (Fig. 4C). Cells transfected with *AsefΔAPC* were also substantially larger than the parental cells and exhibited a morphology very similar to that of the *Asef*- and *APC-arm*–transfected cells (Fig. 4E). In contrast, the AsefΔAPC mutant also lacking the DH domain did not show such activity (*9*). Both Asef and AsefΔAPC localized in the cytoplasm and concentrated in membrane ruffles and at the edges of cells not in contact with other cells (Fig. 4, A, C, and E). Staining with anti-APC revealed that both endogenous APC and exogenously expressed APC-arm colocalized with Asef (Fig. 4, A to D). In cells not transfected with *Asef*, APC concentrated near the margin of protruding membrane structures as reported previously (*22*). However, these clusters of APC were not detected in *Asef*-transfected cells. These results suggest that Asef acts as a GEF for Rac in living cells and that its activity is regulated by APC.

Many members of the Dbl family are oncogenic, especially when truncated (*8*). However, neither the full-length nor NH_2-terminal–truncated derivatives of Asef show any oncogenic activity (*9*).

The armadillo repeat domain is the most highly conserved feature in APC, suggesting that it is essential for function (*1*, *23*). We have demonstrated here that the armadillo repeat domain of APC interacts with a Rac-specific GEF, Asef, and activates its activity. These findings raise the possibility that APC plays a role in regulating the actin cytoskeletal network, thereby affecting cell morphology, polarity, and migration. Indeed, it has been suggested that APC may be involved in epithelial cell migration (*22*, *24*). Furthermore, the colocalization of Asef and APC at the synapse of neuronal cells suggests that this complex is involved in signal transduction at the synapse in addition to neuronal cell migration. However, the identity of the signal that regulates the function of the APC-Asef complex in colon epithelial cells and neuronal cells remains to be elucidated.

Many of the mutant APCs found in colon cancers lack binding sites for microtubules, hDLG, and some of the β-catenin–binding sites, although the armadillo repeat domain itself is not always deleted (*1*). It is therefore interesting to speculate whether the interactions of APC with these proteins are important for localizing Asef to sites where it can properly exert its effect on the actin cytoskeletal network. Consistent with this, we found that the Asef-APC complex is associated with β-catenin. Thus, when Asef binds to mutant APCs, it may fail to be properly localized, thereby compromising its ability to stimulate migration of colon epithelial cells. This abrogation of Asef function could promote tumorigenesis by increasing the accumulation of proliferating cells in the intestinal crypt.

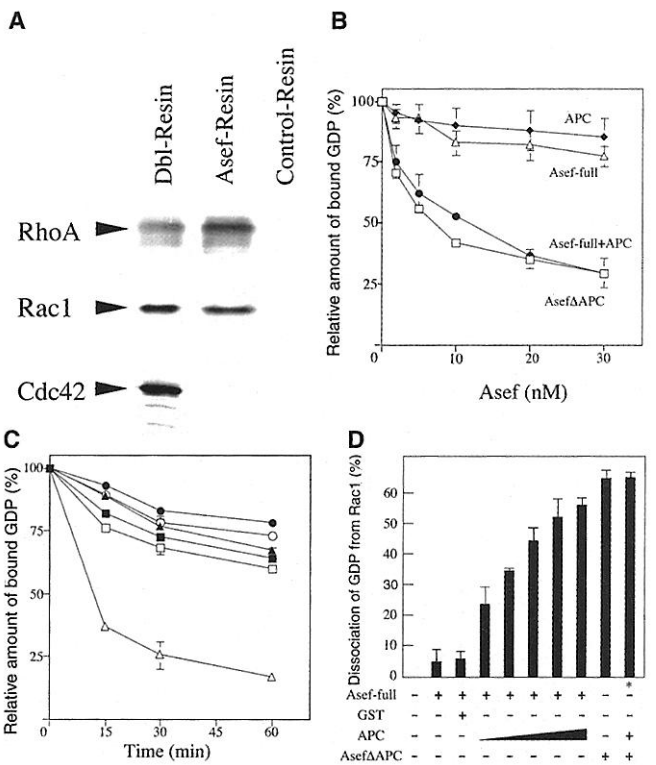

Fig. 3. Stimulation of Asef guanine nucleotide exchange activity by APC. (**A**) Binding of Asef to Rho family guanosine triphosphatases. His_6-AsefΔAPC bound to ProBand Resin was incubated with RhoA, Rac1, or GST-Cdc42. The bound proteins were subjected to immunoblot analysis. As a negative control, ProBand Resin that had not been incubated with Asef was used. (**B**) Dissociation of [^{3}H]GDP from Rac1 (20 nM) after 15 min of incubation at 30°C in the absence or presence of APC-arm (100 nM) and/or the indicated concentrations of Asef or AsefΔAPC (*19*). The amount of [^{3}H]GDP remaining bound to Rac1 was determined, and results are expressed as percentages of the values obtained in the absence of Asef and APC. (**C**) Time course of [^{3}H]GDP dissociation from Rac1 (triangles), RhoA (squares), and Cdc42 (circles) (20 nM) was measured at 30°C in the absence (closed symbols) or presence (open symbols) of AsefΔAPC (20 nM). At the indicated times, portions of the incubation mixture were removed, and the amount of [^{3}H]GDP remaining bound to Rac1, RhoA, and Cdc42 was determined. Results are expressed as percentages of the values obtained at 0 min. (**D**) Dissociation of [^{3}H]GDP from Rac1 (20 nM) after 15 min of incubation at 30°C in the absence or presence of GST (100 nM), Asef (20 nM), AsefΔAPC (20 nM), and/or the various concentrations of APC-arm (10, 20, 40, 100, 200 nM). (*) APC-arm (100 nM) was used.

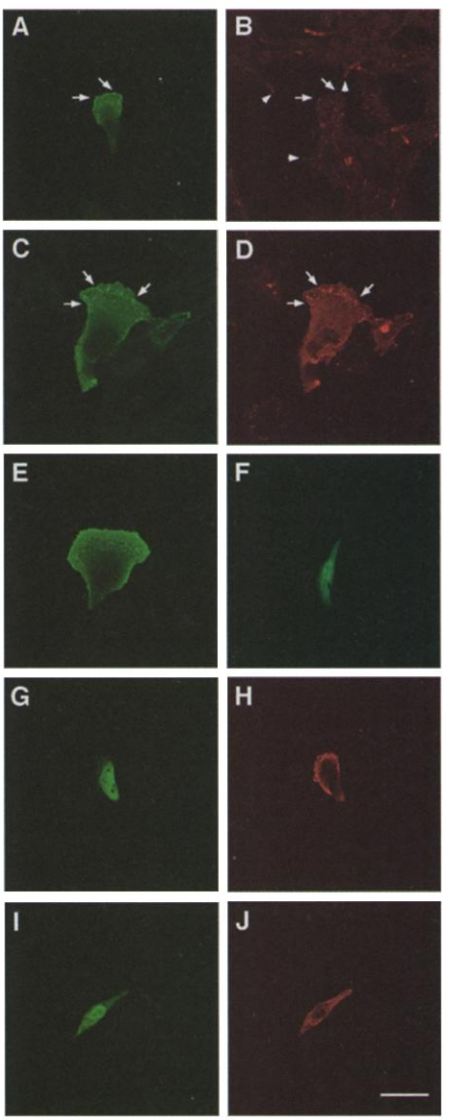

Fig. 4. Morphology of MDCK cells transfected with *Asef*. MDCK cells were transfected with expression plasmids encoding HA-tagged Asef (**A** and **B**), HA-tagged Asef and Myc-tagged APC-arm (**C** and **D**), HA-tagged AsefΔAPC (**E**), Myc-tagged APC-arm (**F**), HA-tagged Asef and GFP (**G** and **H**), or HA-tagged Asef and the APC-binding region of Asef (ABR in Fig. 2A) fused to GFP (GFP-ABR) (**I** and **J**). MDCK cells were double-stained with antibodies against HA (A, C, E, H, and J), APC (B), and Myc (D and F). GFP (G) and GFP-ABR (I) were visualized as green fluorescence. Arrowheads in (B) point to clusters of APC in extending membranes, and arrows in (A) to (D) indicate areas of colocalization of Asef and APC. Bar, 50 μm.

References and Notes

1. K. W. Kinzler and B. Vogelstein, *Cell* **87,** 159 (1996); P. Polakis, *Biochim. Biophys. Acta* **1332,** F127 (1997); M. Bienz, *Curr. Opin. Genet. Dev.* **9,** 595 (1999).
2. G.-H. Baeg *et al.*, *EMBO J.* **14,** 5618 (1995).
3. B. Rubinfeld *et al.*, *Science* **262,** 1731 (1993); L.-K. Su, B. Vogelstein, K. W. Kinzler, *Science* **262,** 1734 (1993); J. R. Miller and R. T. Moon, *Genes Dev.* **10,** 2527 (1996); K. M. Cadigan and R. Nusse, *Genes Dev.* **11,** 3286 (1997).
4. J. Behrens *et al.*, *Science* **280,** 596 (1998); S. Ikeda *et al.*, *EMBO J.* **17,** 1371 (1998); T. Nakamura *et al.*, *Genes Cells* **3,** 395 (1998); M. J. Hart, R. de los Santos, I. N. Albert, B. Rubinfeld, P. Polakis, *Genes Cells* **8,** 573 (1998); F. Hamada *et al.*, *Science* **283,** 1739 (1999).
5. L.-K. Su *et al.*, *Cancer Res.* **55,** 2972 (1995).
6. A. Matsumine *et al.*, *Science* **272,** 1020 (1996).
7. The plasmid GBT9-APC, which encodes the GAL4 DNA-binding domain fused to the armadillo repeat domain of human APC (amino acids 446 to 880), was used as target in two-hybrid screens of a human fetal brain cDNA library (Clontech). Seven clones containing a fragment of the Asef cDNA were obtained from 1.1×10^7 transformants. The remaining 5′- and 3′-end regions were obtained by the 5′ and 3′ rapid amplification of cDNA ends (RACE) systems, respectively, with the "Marathon"-ready human brain cDNA (Clontech).
8. R. A. Cerione and Y. Zheng, *Curr. Opin. Cell Biol.* **8,** 216 (1996); I. P. Whitehead, S. Campbell, K. L. Rossman, C. J. Der, *Biochem. Biophys. Acta* **1332,** F1 (1997).
9. Y. Kawasaki *et al.*, unpublished data.
10. The ^{35}S-methionine–labeled armadillo repeat domain of APC and Asef−M were synthesized by use of the coupled transcription-translation TNT system (Promega). GST and GST-fusion proteins (2 μg) immobilized to glutathione-Sepharose beads were mixed with in vitro–translated proteins in binding buffer [20 mM tris-HCl (pH 8.0), 140 mM NaCl, 1 mM EGTA, 1 mM dithiothreitol (DTT), 10% glycerol, 1% Triton X-100, aprotinin (10 μg/ml), leupeptin and pepstatin] for 1 hour at 4°C. After five washes with binding buffer, bound proteins were fractionated by SDS–polyacrylamide gel electrophoresis (PAGE) followed by autoradiography.
11. Antibodies to Asef were prepared by immunizing rabbits with a peptide containing amino acids 73 to 126 of Asef. Antibodies to APC were prepared by immunizing rabbits with a peptide containing amino acids 1122 to 1729 of APC. Mouse monoclonal antibody (mAb) to APC was raised against the COOH-terminal 15 amino acids of APC. Antibodies were purified by affinity chromatography with columns to which the antigens used for immunization had been linked. Mouse mAbs to β-catenin and the hemagglutinin (HA) tag (12CA5) were from Transduction Laboratories and Boehringer, respectively. Rabbit polyclonal antibody to the Myc tag (polyclonal version of 9E10) was from MBL. Immunoprecipitation was performed as in (*6*). Immunoblotting analysis was performed with alkaline phosphatase–conjugated mouse anti-rabbit immunoglobulin G (IgG) or goat anti-mouse IgG (Promega) as a second antibody. On the basis of the immunoblotting and immunoprecipitation experiments, we estimate that about 10 to 20% of Asef and APC are included in the Asef-APC complex (*9*).
12. Supplemental Web material is available at *Science* Online at www.sciencemag.org/feature/data/1049013.shl.
13. Serial frozen sections of mouse colon and brain were stained with anti-APC or anti-Asef and visualized by incubation with avidin-biotin-peroxidase complex (*14*).
14. T. Senda *et al.*, *Neuroscience* **83,** 857 (1998).
15. J. S. Brakeman, S. H. Gu, X. B. Wang, G. Dolin, J. M. Baraban, *Neuroscience* **91,** 661 (1999).
16. Double-labeling immunoelectron microscopy was performed with rabbit anti-Asef and mouse mAb to APC as in (*6*).
17. His_6-AsefΔAPC bound to ProBond Resin (Invitrogen) was mixed with RhoA, Rac1, and GST-Cdc42 in buffer A [50 mM Hepes (pH 7.0), 150 mM NaCl, 50 mM NaF, 5 mM EDTA, 1 mM DTT, phenylmethylsulphonyl fluoride (50 μg/ml), leupeptin (1 μg/ml), and aprotinin (1 μg/ml)] containing 0.1% NP-40 for 1 hour at 4°C and then washed extensively with buffer A. Proteins adhering to the resin were analyzed by 13% SDS-PAGE and subjected to immunoblotting. Mouse mAb to Rac1 was from Transduction Laboratories. Rabbit polyclonal antibodies to Cdc42Hs and mouse mAb to RhoA were from Santa Cruz.
18. T. Miki, C. L. Smith, J. E. Long, A. Eva, T. P. Fleming, *Nature* **362,** 462 (1993).
19. The [^{3}H]GDP-bound form of Rac1 was obtained by incubating 2 pmol of Rac1 with 0.2 μM [^{3}H]GDP for 20 min at 30°C in 20 mM tris-HCl (pH 8.0), 3 mM $MgCl_2$, 10 mM EDTA, and 1 mM DTT. To prevent dissociation of [^{3}H]GDP from Rac1, we added 375 mM $MgCl_2$ to a final concentration of 18 mM, and the mixtures were immediately cooled on ice. Dissociation of [^{3}H]GDP was measured at 25°C in 20 mM tris-HCl (pH 8.0), 6 mM $MgCl_2$, 3.5 mM EDTA, and 1 mM DTT by addition of a 250-fold excess of unlabeled GDP, GTP, and the indicated amounts of Asef. The reaction was stopped by addition of 1 ml of ice-cold stop buffer [20 mM tris-HCl (pH 8.0), 25 mM $MgCl_2$, and 100 mM NaCl]. The diluted mixtures were passed through nitrocellulose filters, the filters were washed several times with stop buffer, and the trapped radioactivity was counted.
20. L. Van Aelst and C. D'Souza-Schorey, *Genes Dev.* **11,** 2295 (1997); A. Hall, *Science* **279,** 509 (1998).
21. Canine kidney epithelial MDCK cells were cultured in Dulbecco's modified Eagle's medium supplemented with 10% fetal calf serum. Plasmids encoding HA-tagged Asef, HA-tagged AsefΔAPC, Myc-tagged APC-arm, green fluorescent protein (GFP), and GFP-ABR were subcloned into pcDNA3.1(+) and transfected into MDCK cells with LipofectAMINE (Life Technologies). Cells were double-stained with antibodies against HA, Myc, and APC. Staining patterns obtained with anti-HA were visualized with fluorescein isothiocyanate–labeled anti-rabbit IgG; those obtained with anti-Myc and anti-APC were visualized with rhodamine-labeled anti-mouse IgG. The cells were photographed with a Carl Zeiss LSM510 laser-scanning microscope.
22. I. S. Nathke, C. L. Afams, P. Polakis, J. H. Sellin, W. J. Nelson, *J. Cell Biol.* **134,** 165 (1996).
23. H. Nakagawa *et al.*, *Cancer Res.* **58,** 5176 (1998); J. H. van Es *et al.*, *Curr. Biol.* **9,** 105 (1999); X. Yu, L. Waltzer, M. Bienz, *Nature Cell Biol.* **1,** 144 (1999); F. Hamada *et al.*, *Genes Cells* **4,** 465 (1999); B. M. McCartney *et al.*, *J. Cell Biol.* **146,** 1303 (1999).
24. M. H. Wong, M. L. Hermiston, A. J. Syder, J. I. Gordon, *Proc. Natl. Acad. Sci. U.S.A.* **93,** 9588 (1996).

25. We thank Y. Takai for recombinant Rac1, Rho, and Cdc42; K. Kohno and M. Kurimoto for mouse mAbs to APC; and M. Lamphier for reading the manuscript. Supported by Grants-in-Aid for Scientific Research on Priority Areas and the Organization for Pharmaceutical Safety and Research.

28 January 2000; accepted 6 July 2000

Genes Expressed in Human Tumor Endothelium

Brad St. Croix,[1] Carlo Rago,[1,2] Victor Velculescu,[1] Giovanni Traverso,[1] Katharine E. Romans,[3] Elizabeth Montgomery,[3] Anita Lal,[4] Gregory J. Riggins,[4] Christoph Lengauer,[1] Bert Vogelstein,[1,2] Kenneth W. Kinzler[1]*

To gain a molecular understanding of tumor angiogenesis, we compared gene expression patterns of endothelial cells derived from blood vessels of normal and malignant colorectal tissues. Of over 170 transcripts predominantly expressed in the endothelium, 79 were differentially expressed, including 46 that were specifically elevated in tumor-associated endothelium. Several of these genes encode extracellular matrix proteins, but most are of unknown function. Most of these tumor endothelial markers were expressed in a wide range of tumor types, as well as in normal vessels associated with wound healing and corpus luteum formation. These studies demonstrate that tumor and normal endothelium are distinct at the molecular level, a finding that may have significant implications for the development of anti-angiogenic therapies.

Tumors require a blood supply for expansive growth (*1–3*), an observation that has stimulated a profusion of research on tumor angiogenesis. However, several basic questions about tumor vessels remain unanswered. For example, is endothelium that lines blood vessels in tumors qualitatively different from endothelium in vessels of normal tissue? What is the relation of tumor angiogenesis to angiogenesis associated with wound healing or other physiological processes? The answers to these questions critically impact the potential for new therapeutic approaches to inhibit angiogenesis in a tumor-specific manner.

To determine if tumor-specific endothelial markers exist, we compared gene expression profiles in endothelium derived from normal and tumor tissue. Human colorectal cancer was chosen for these studies because it has a high incidence, tends to grow slowly, and is often resistant to chemotherapeutic drugs. Importantly, the progressive growth of this tumor type appears to be angiogenesis-dependent (*4*).

Global analysis of gene expression in tumor and normal endothelium is difficult be-

[1]Johns Hopkins Oncology Center, [2]Howard Hughes Medical Institute, [3]Department of Pathology, Johns Hopkins University School of Medicine, Baltimore, MD 21231, USA. [4]Department of Pathology, Duke University Medical Center, Durham, NC 27710, USA.

*To whom correspondence should be addressed. E-mail: kinzlke@jhmi.edu